

Influence of admixtures, external magnetic field and neon plasma sheath with deuterium gas-puff on the neutron production in plasma focus discharges

P. Kubes¹, M. Paduch², E Zielinska², E. Kowalska-Strzeciwiłk², M Scholz³,
L. Karpinski⁴, J. Cikhardt¹, D. Klir¹, J. Kravarik¹, J. Kortanek¹, K. Rezac¹

¹Czech Technical University Prague, Czech Republic

²Institute of Plasma Physics and Laser Microfusion Warsaw, Poland

³Institute of Nuclear Physics, Krakow, Poland

⁴Rzeszow University of Technology, Rzeszow, Poland

Outline

Experiments and results provided on PF-1000 in 2012-13

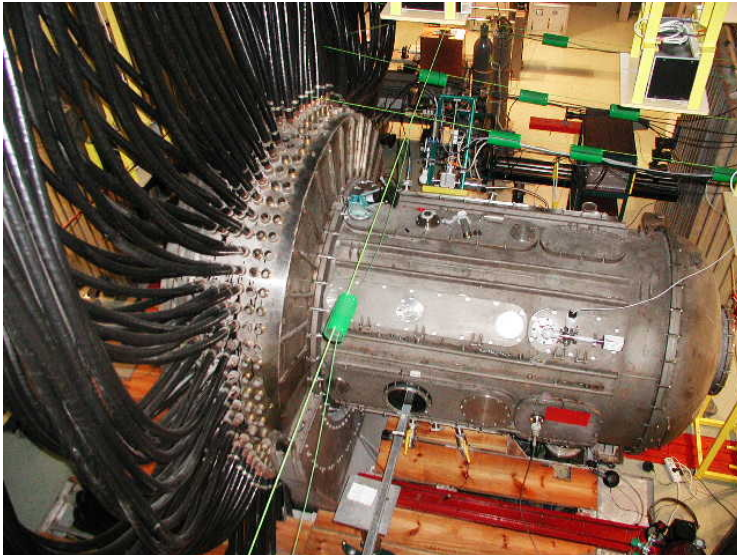
1. Influence of the tungsten anode face on the neutron production and X-ray radiation
2. Influence of the external poloidal magnetic field on the neutron production and X-ray radiation
3. Compression of the deuterium from the gas-puff in the anode by the neon plasma sheath

PF-1000 IPPLM Warsaw, Poland

2 MA, 400 kJ, D-D reaction, D₂ gas

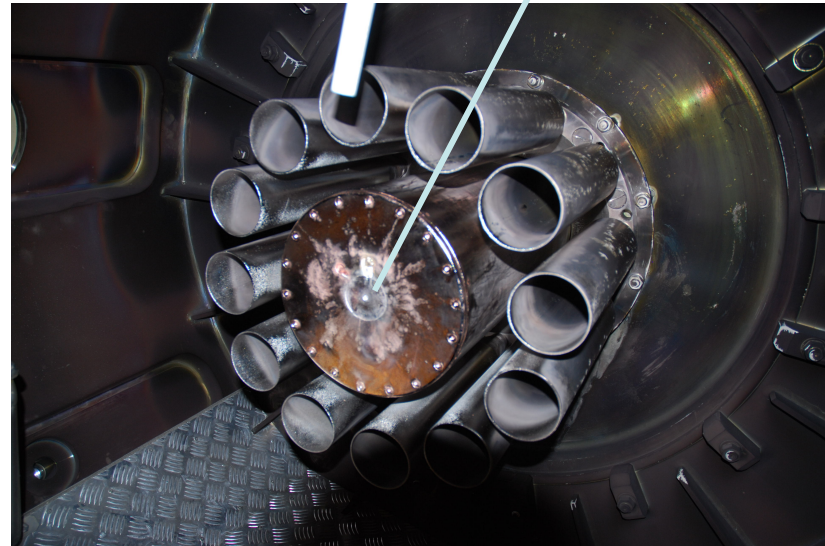
neutron yield 10¹⁰-10¹² , horizontal position of discharge axis

facility



electrode system

tungsten plate



the intense neutron source

Scintillation detectors of neutrons in axial and radial directions

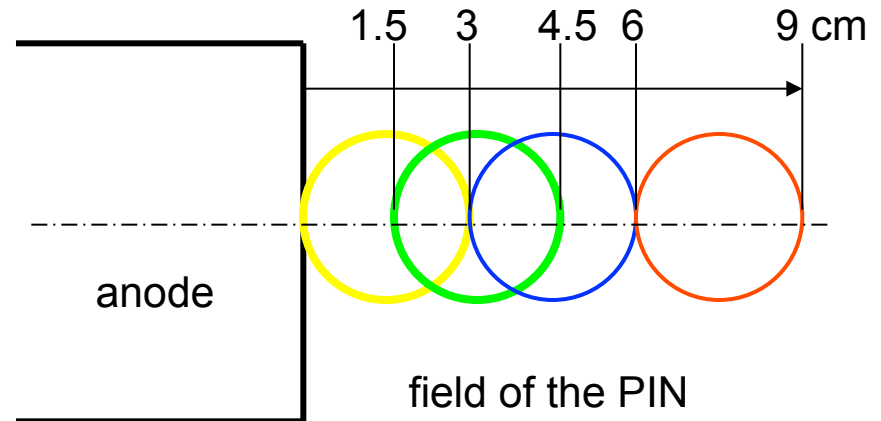
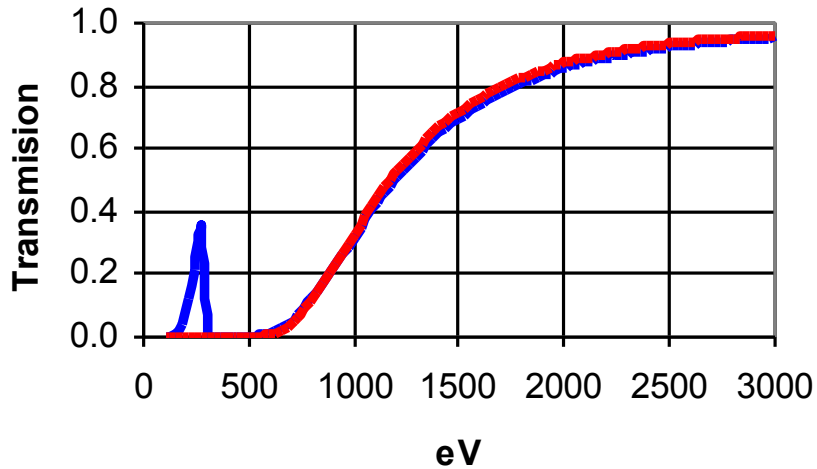
Mach-Zender interferometer, 16 beams, 527 nm, 1 ns during 220 ns

signals of U,I,dI,

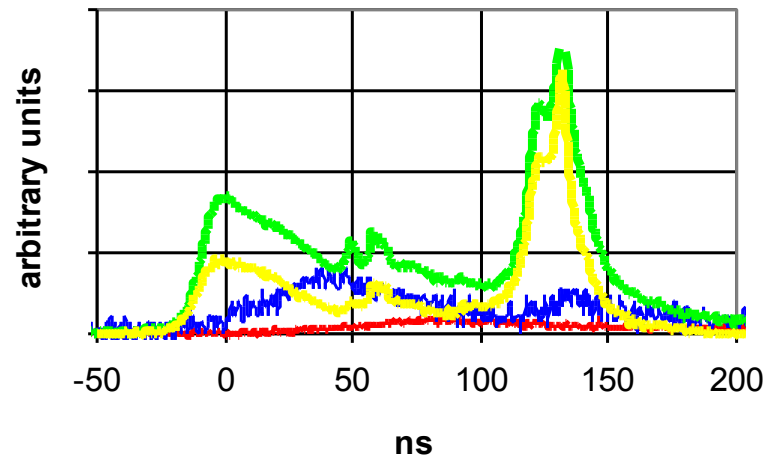
Soft X-frames + MCP+CCD

4 Soft X PIN

Soft X-ray diagnostics



X-frames - transmission of polystyrene 5 μm
PIN detectors Be 10 μm filters
Window 150-300 eV
The same sensitivity 0.7-5 keV

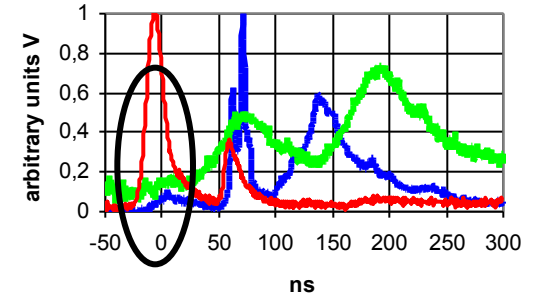
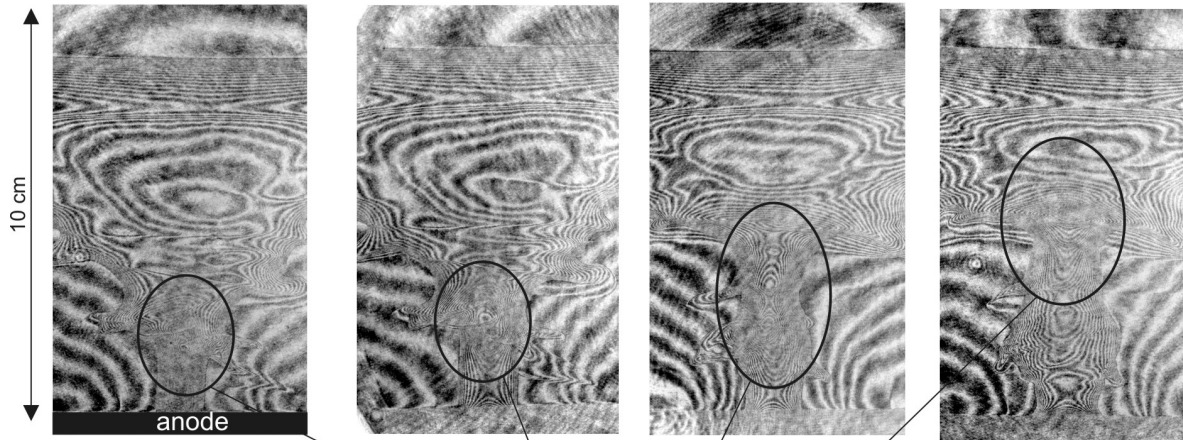


sensitivity of PIN

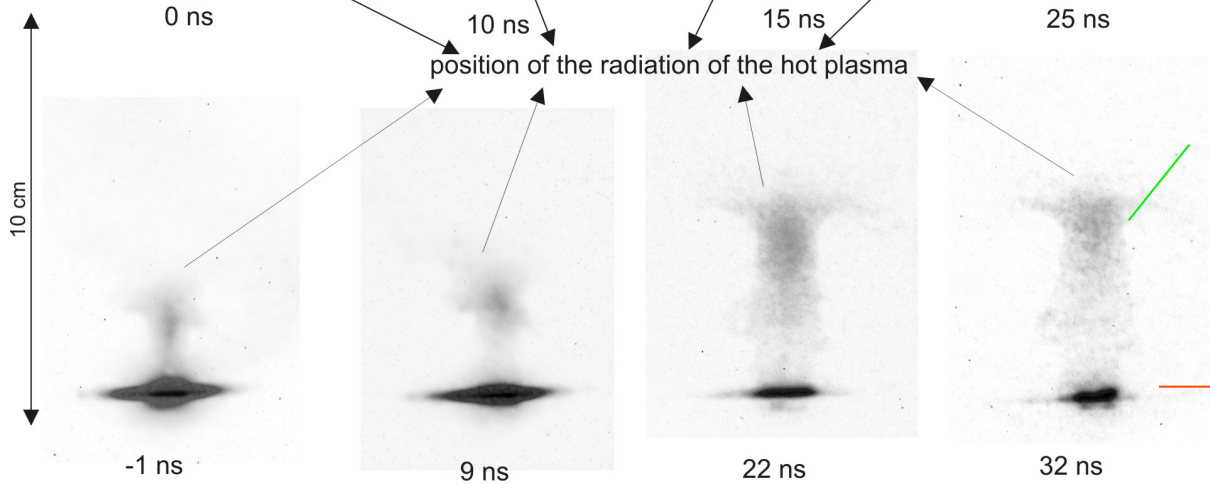
Tungsten anode plate - first neutron pulse

Shot # 9748

Shot # 9761



Signals **SXR**, **HXR**, neutrons
Time 0 - current derivative dip

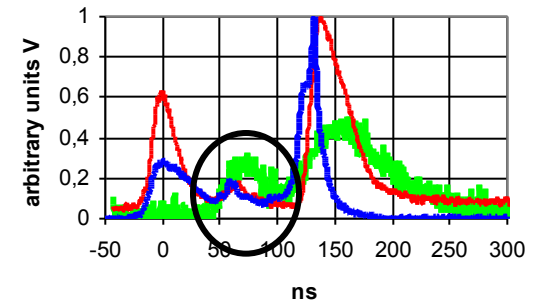
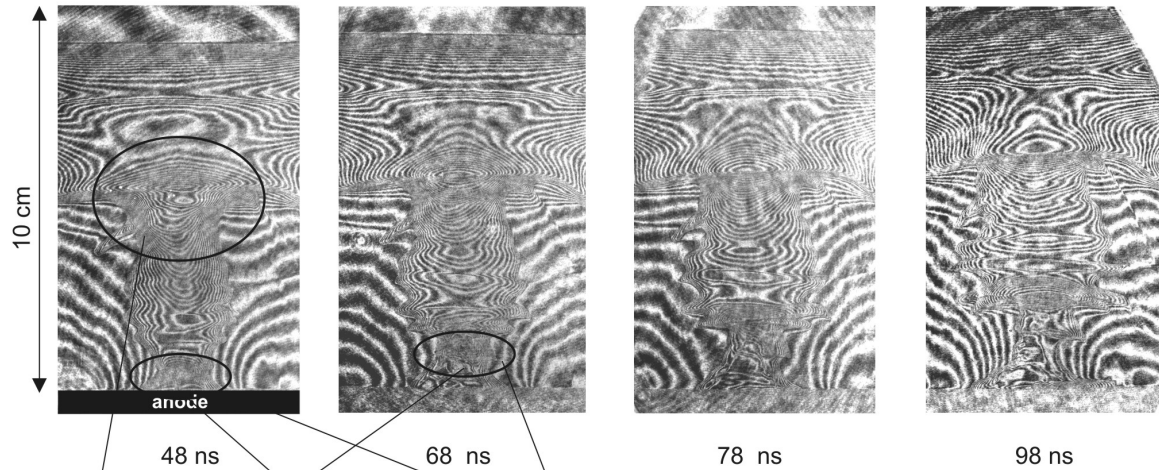


Bremsstrahlung from the deuterium plasmoid

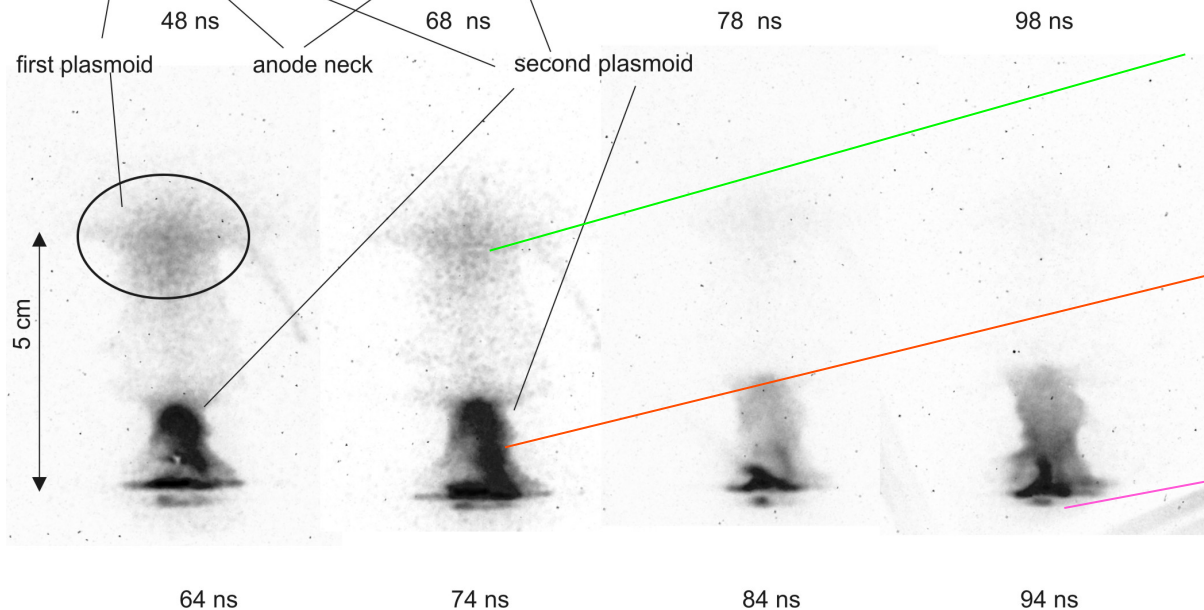
Recombination from the anode

Evolution of anode constriction in plasma with tungsten

Shot # 9755



Signals **SXR**, **HXR**, **neutrons**



Bremsstrahlung from the deuterium plasmoid

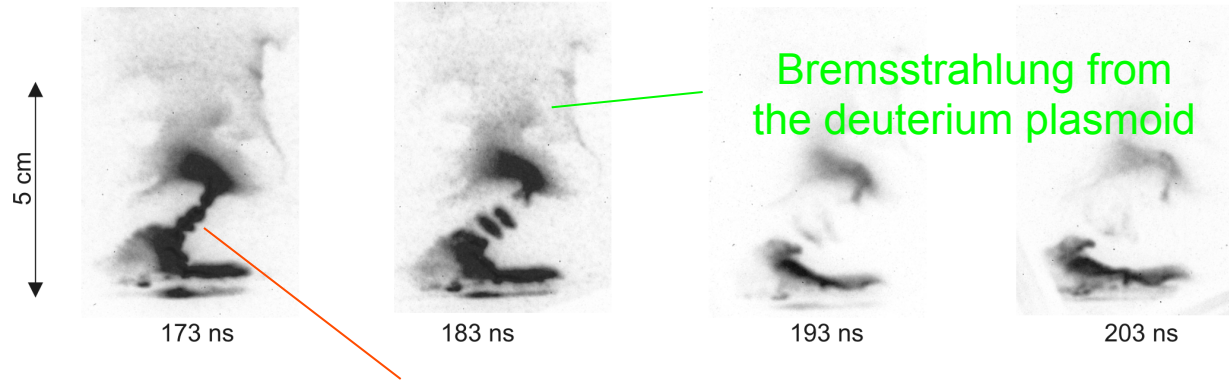
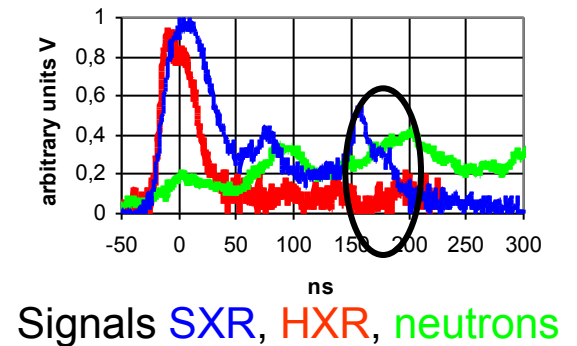
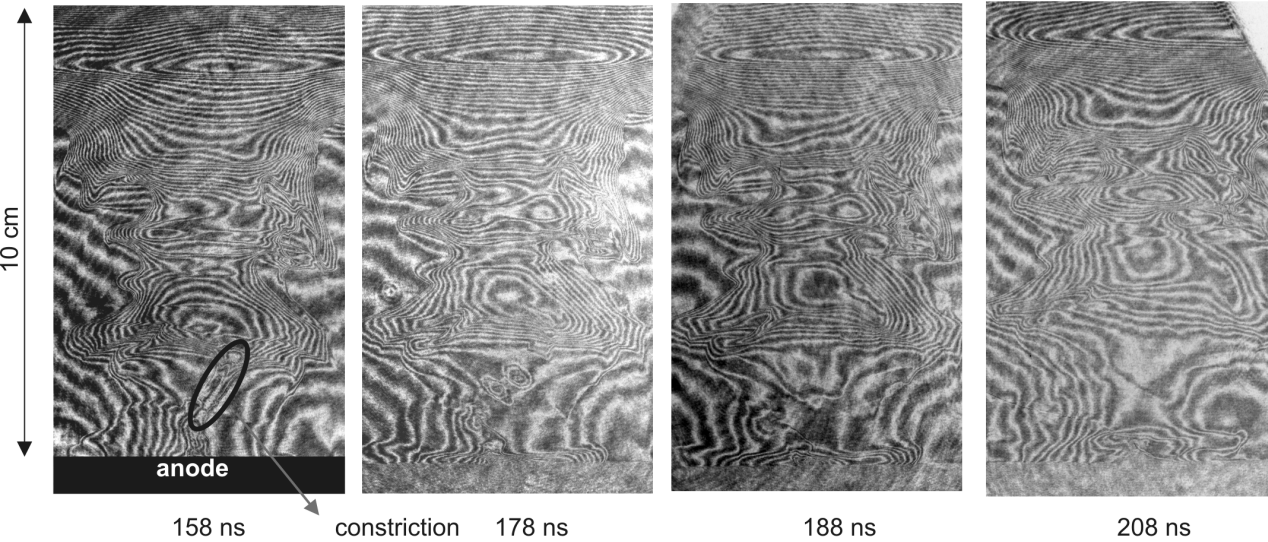
Recombination from the anode constriction

Recombination from the anode

Transport of tungsten into plasma column due to constriction
 „wall instability“ *Bride R D et al 2013 Phys. Plasmas* **20**, 059309

Evolution of constriction in plasma with tungsten

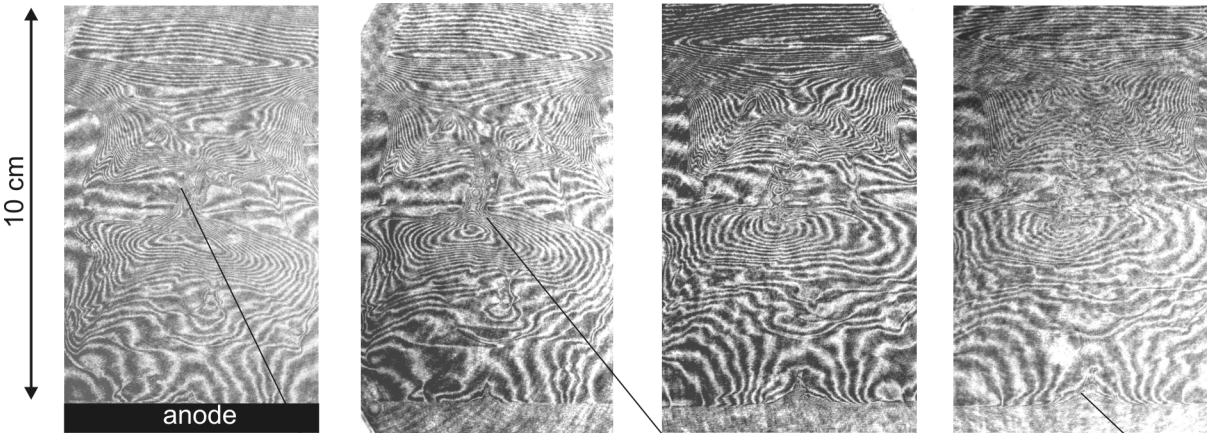
9762



Emission of the region of the decay of constriction and of the ejected plasma

Evolution of constriction in plasma without tungsten

Shot # 9754

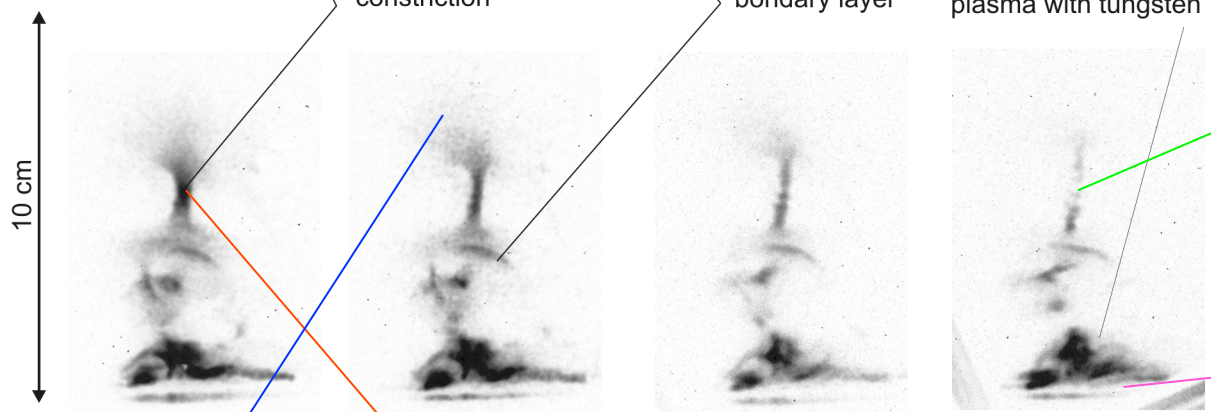


149 ns

159 ns

179 ns

189 ns



151 ns

161 ns

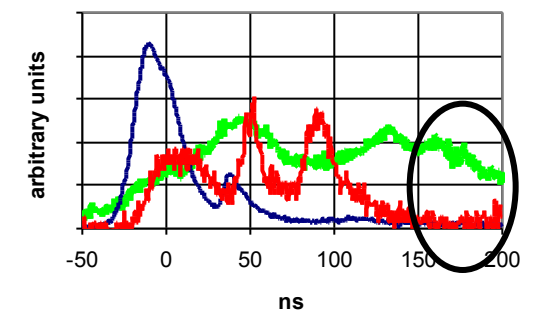
171 ns

181 ns

constriction

boundary layer

plasma with tungsten



Signals **SXR**, **HXR**, **neutrons**

Bremsstrahlung from the deuterium plasmoid

Recombination from the anode

Hot plasma in the constriction without tungsten
Colder plasma in region of ejected plasma

Power of recombination and bremsstrahlung

Artsimovich L A, Sagdeev R Z 1979 *Plasma Physics for Physicists*; Moscow - Atomizdat

recombination $R_R = 5 \times 10^{-33} z_W^4 n_e n_W T_e^{-1/2}$

bremstrahlung $R_B = 1.5 \times 10^{-38} z_D^2 n_e n_D T_e^{+1/2}$

ratio $\frac{R_R}{R_B} = 3.3 \times 10^5 \frac{z_W^4}{z_D^2} \frac{n_W}{n_D} T_e^{-1}$

[m³, K]

Deuterium bremsstrahlung dominates at $T_e \geq 30$ eV

Recombination of tungsten dominates for 1%, T_e 30-100 eV, $z \approx 3-6$

Conclusions

In pure deuterium dominates bremsstrahlung namely in the last phase of the existence of the compact constriction

Recombination dominates in the region with tungsten during evolution of instabilities (2 times higher power in comparison with bremsstrahlung in pure deuterium Estimations 1% of W, $z \approx 3-4$)

Recombination increases during decay of the constriction – analogy of hot spots at higher z

Decrease of the neutron yield to 40% and decrease of the energy of fast deuterons producing neutrons to 80%

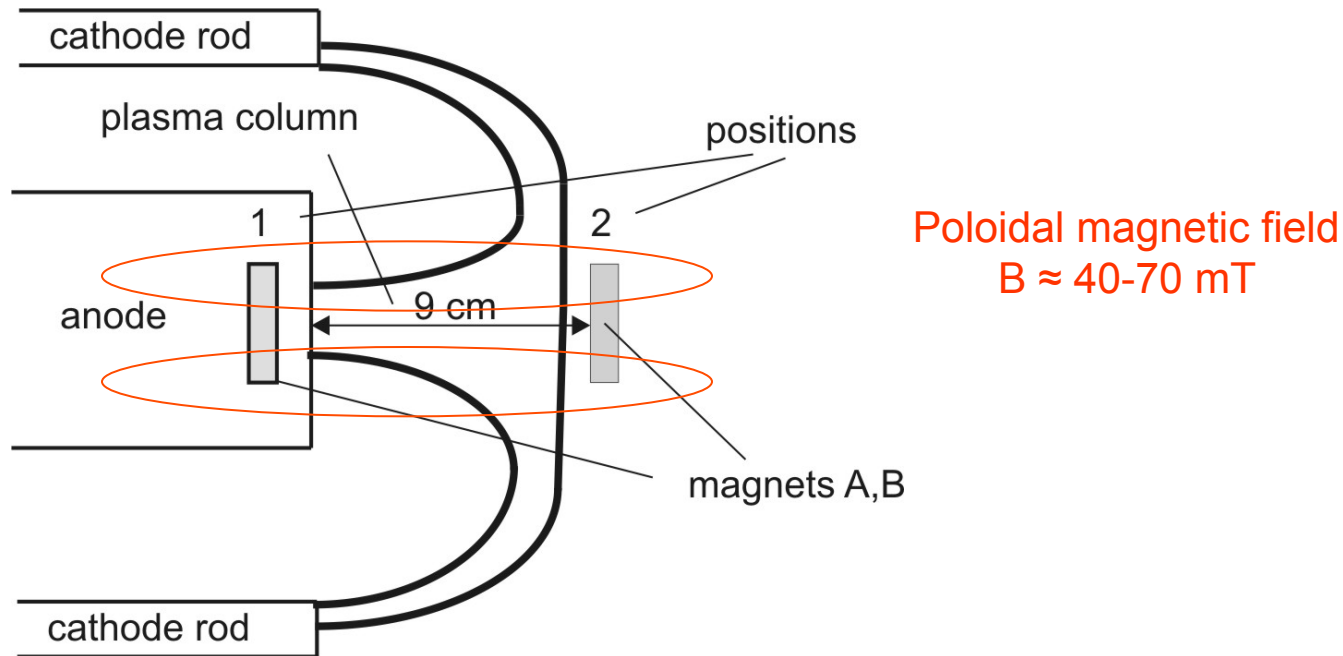
At presents of tungsten – decrease of implosion velocity of constriction from 2.5×10^5 m/s to $1-2 \times 10^5$ m/s

At this implosion, energy of 10-40 keV delivered to the tungsten ions, (whiles to the D ions below 0.5 keV).

Accepted for publication in PPCF

Influence of the external poloidal magnetic field on the neutron production and X-ray radiation

Experiments of M. Paduch and E. Zielinska, IPPLM Warsaw



Compression to the 5-10 T similar as the B_z magnetic field measured by magnetic probes

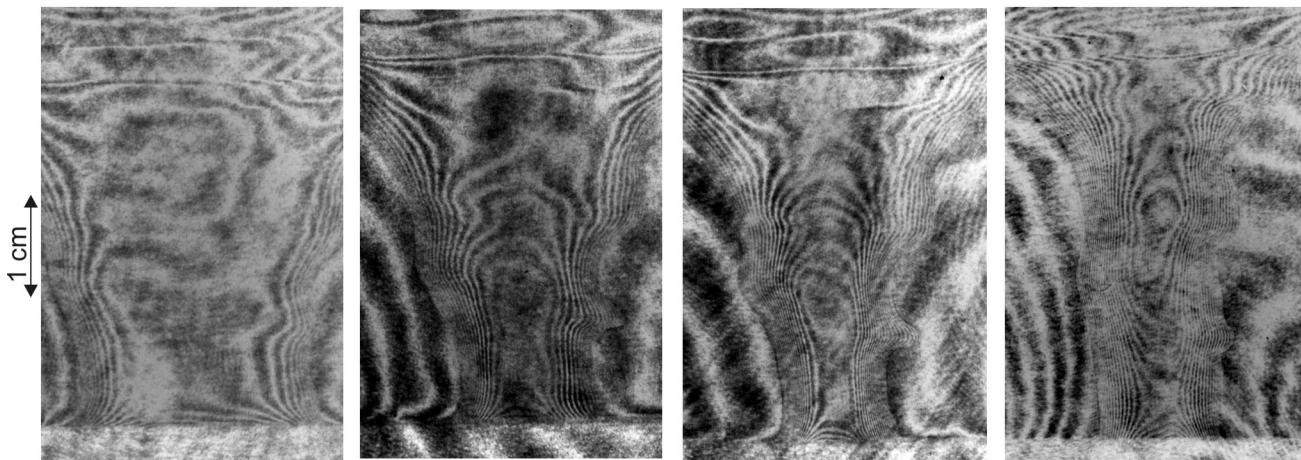
Krauz V I et al 2012 *Plasma Phys. Control. Fusion* **54**, 025010

Krauz V I et al 2012 *Europhys. Lett.* **98**, 45001

First neutron pulse

Shot # 9708

South



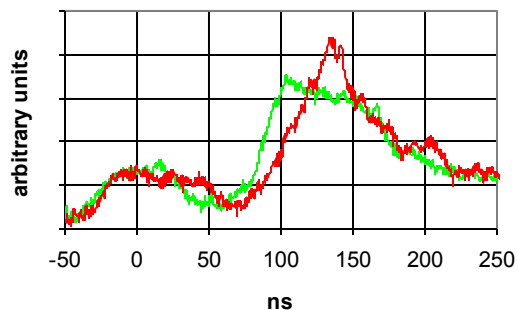
South -40 ns

-20 ns

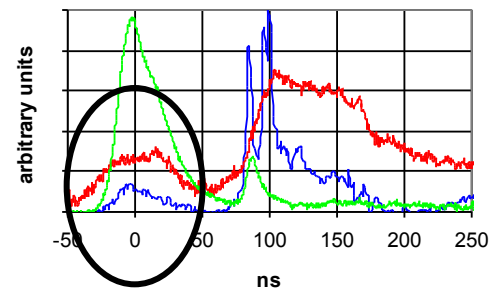
-10 ns

+10 ns

Interferograms at the time of the first neutron pulse



neutron signals registered in
7 m **side-on** and **upstream**



Signals of **PIN**, **HXR** and **neutrons** were registered side-on. Neutrons were temporally shifted to the time of the neutron production using the time-of-flight calculation supposing the neutron energy of 2.45 MeV

Results

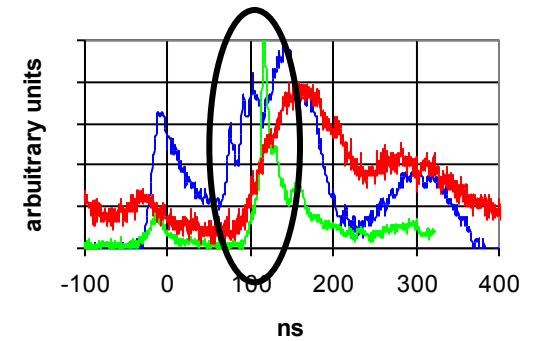
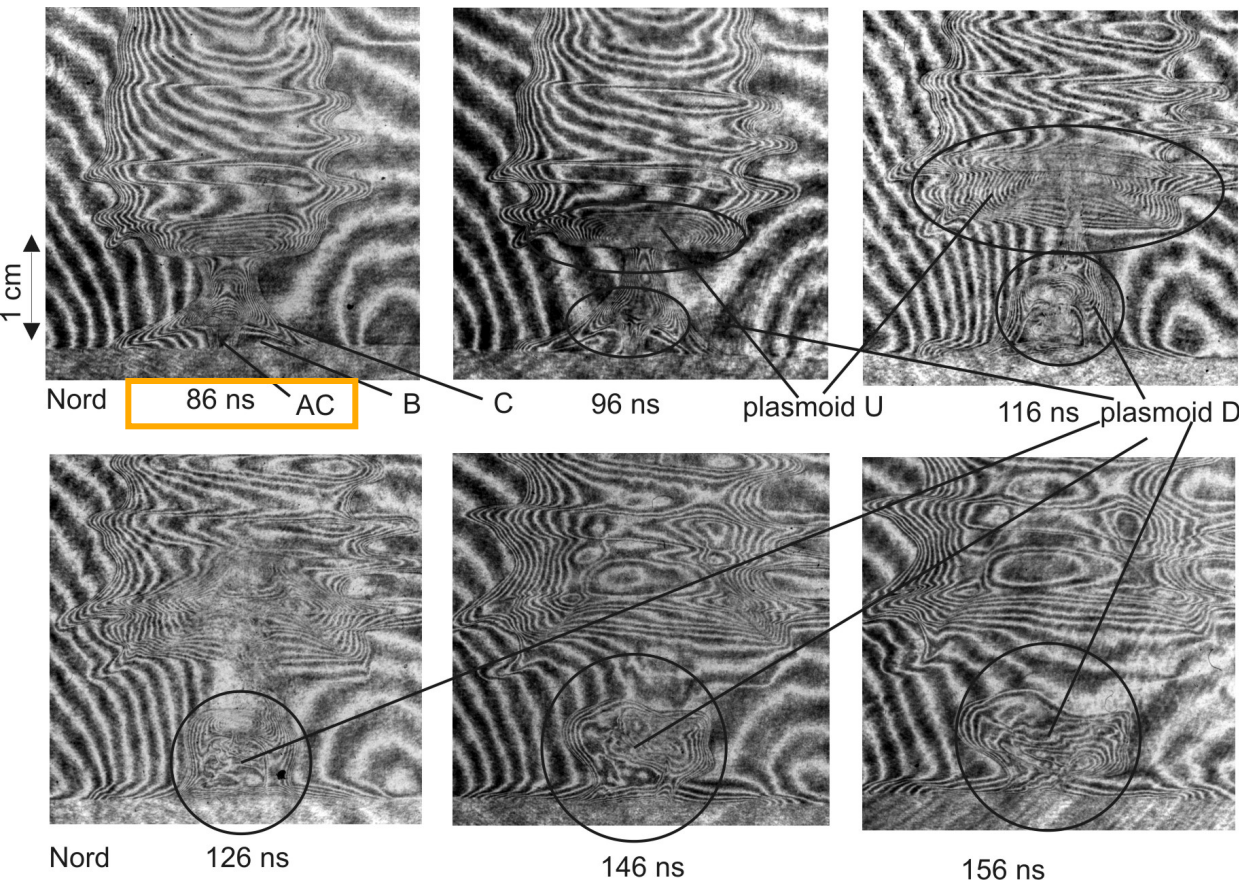
Increase of stability of pinch column

Dominant beam-target mechanism in first neutron pulse

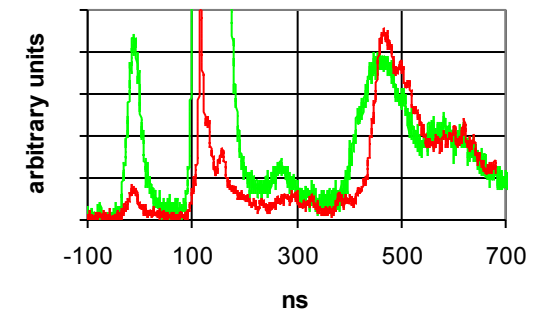
($E_d(z) \approx 100-140$ keV, $E_d(r) \approx 25$ keV)

Magnet in anode – evolution of instability

Shot # 9729



Signals of PIN, HXR and neutrons



HXRs and neutrons registered in 7 m side-on and upstream

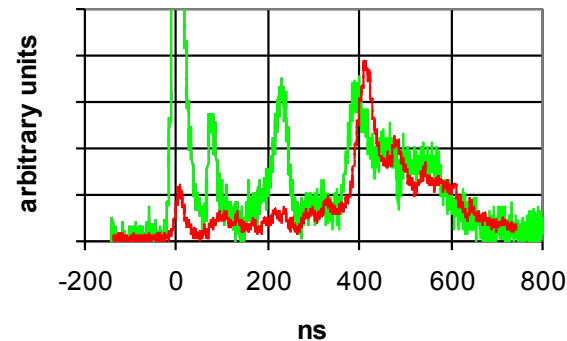
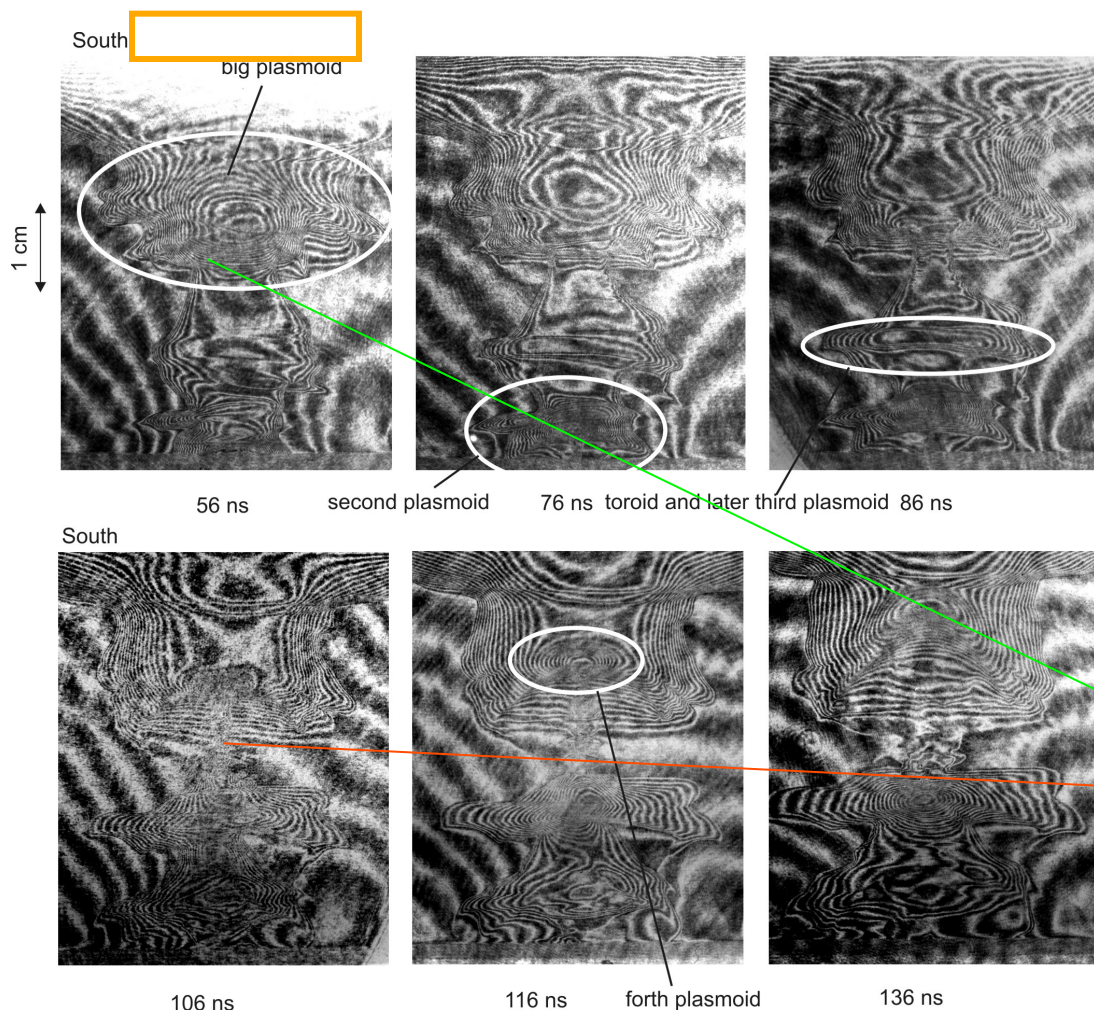
Conclusions:

Decrease of the neutron yield to 40%

Symmetrical column, stable structures

Magnet at end of column – formation of the big plasmoid

Shot # 9716



HXRs and neutrons registered in 7 m **side-on** and **upstream**

Interferograms with **big plasmoid** and **long constriction**

This position of the magnet support formation of the stable and dense target for higher neutron production

Conclusions

At PF-1000 the external poloidal $B_p \approx 40-70$ mT was compressed to the value of 5-8 T, the same value measured by magnetic probes

Magnetic pressure $B_p \approx 1.4 \times 10^7$ Pa 7% of the B_ϕ pressure

Stabilization role:

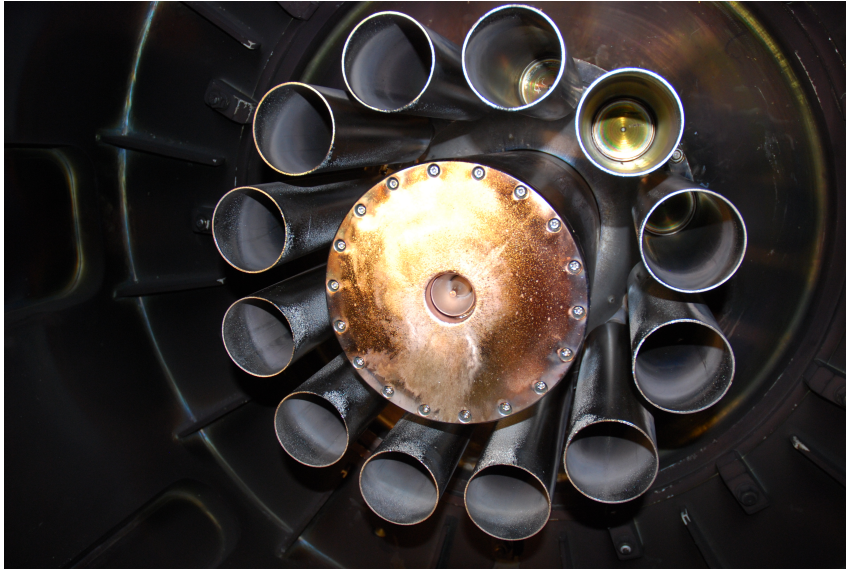
- (i) Decrease of the tearing of B_p
- (ii) Depress of the instabilities on the surface of the plasma column
- (iii) Increase of the symmetry of the column
- (iv) Increase of the length and time-of life of the constriction

external B_p dissipates from the column after 100-150 ns

Possible utilizing:

- (i) Active influence of the optimal internal ratio of B_p/B_t
- (ii) Formation of the stable and dense target for deuteron beams to produce higher neutron yield

Implosion of the deuterium gas-puff by the neon plasma sheath February 2012



Anode \varnothing 23 cm with central nozzle



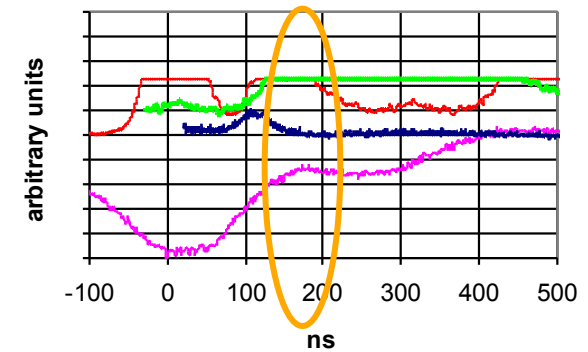
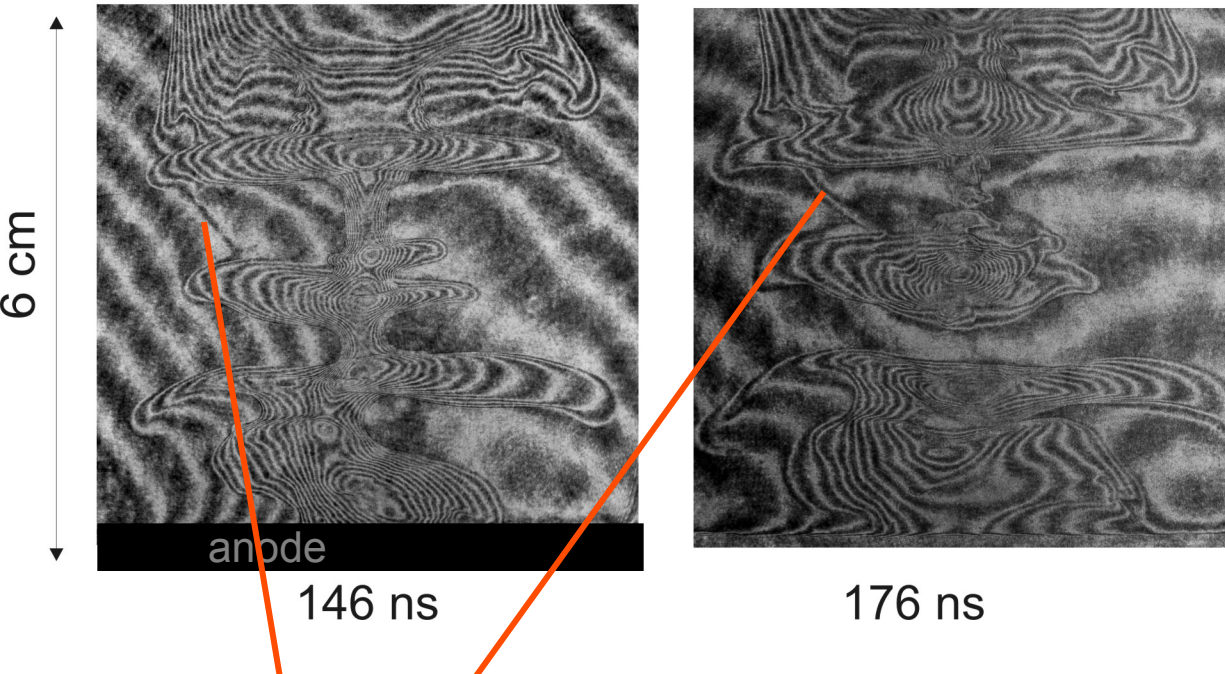
Nozzle \varnothing 4 cm

Experiments:

- (i) Deuterium plasma sheath 1.5 torr, 32 $\mu\text{g}/\text{cm}$
- (ii) Deuterium plasma sheath 32 $\mu\text{g}/\text{cm}$ + deuterium jet 5-10 $\mu\text{g}/\text{cm}$
- (iii) Neon plasma sheath 0.4-0.6 torr, 45 - 65 $\mu\text{g}/\text{cm}$
- (iv) Neon plasma sheath 65 $\mu\text{g}/\text{cm}$ + deuterium jet 5-10 $\mu\text{g}/\text{cm}$

(i) Deuterium plasma sheath 1.5 torr

Shot 9874



SXR, HXR, neutron, dI/dt

Dominant HXR and neutron pulse

Breakdown in the final phase of implosion

Neutron yield 3.3×10^{10} ,

Length of the pinch 7 cm

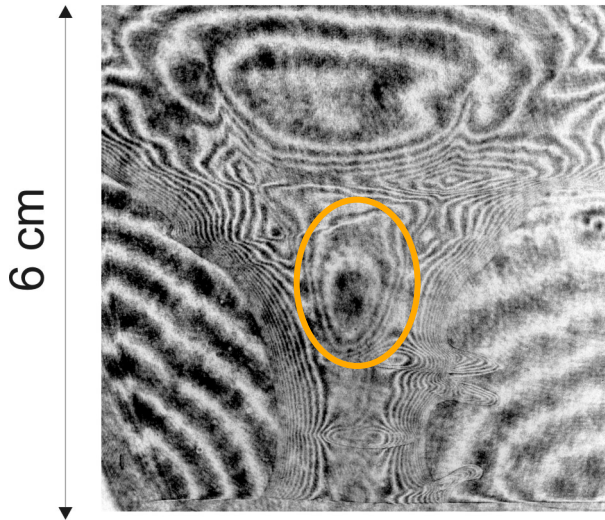
Mean energy of deuterons producing neutrons downstream 160 keV

side-on 70 keV

$n_e \approx n_i$: constriction $3.7 \times 10^{24} \text{ cm}^{-3}$, plasmoid $1.1 \times 10^{24} \text{ cm}^{-3}$; $v \approx 1.6 \times 10^5 \text{ m/s}$

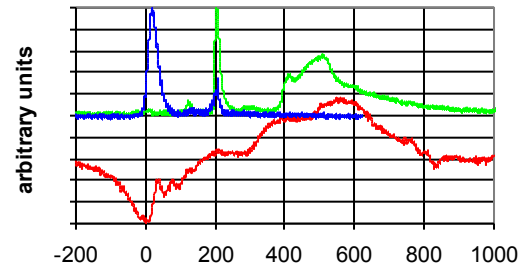
(ii) Deuterium plasma sheath + deuterium jet

Shot 9880

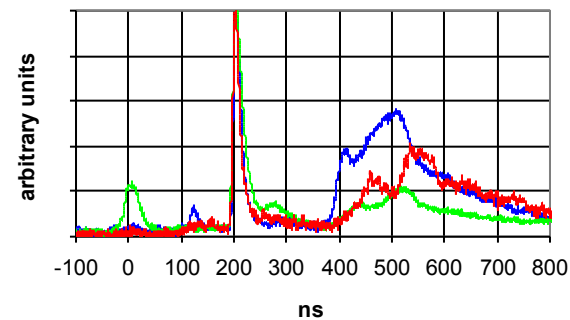


-21 ns

Possibility of estimation of mass
of D from the nozzle $\approx 18\%$



SXR, HXR, neutron, dI/dt

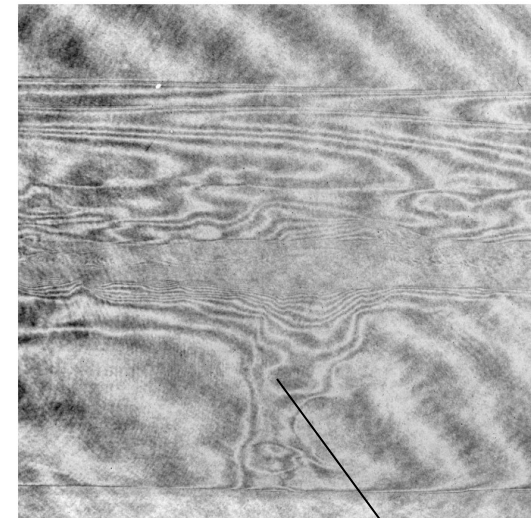
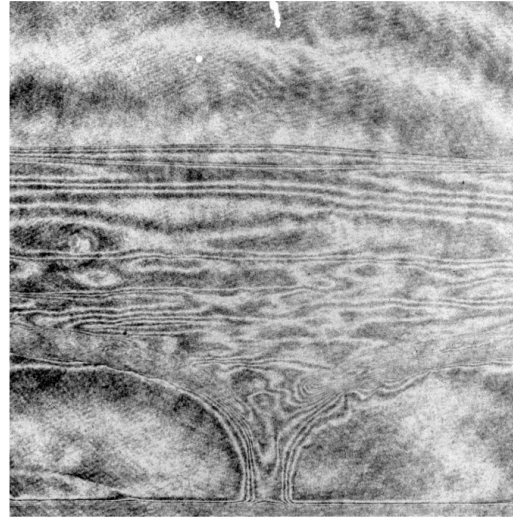
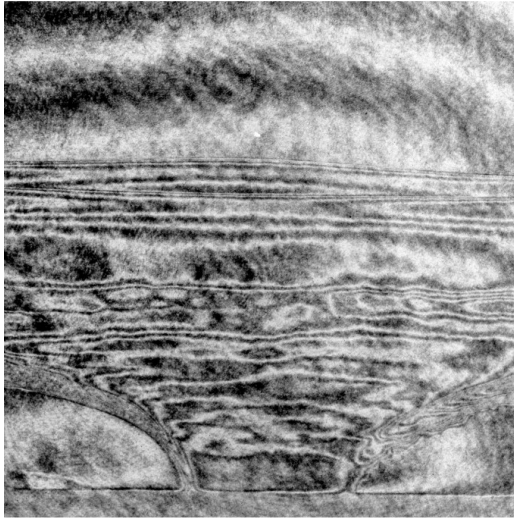


Neutron signals **down**, **side-on** and **up**
 $\Rightarrow E_d(z) \approx 160$ keV, $E_d(r) \approx 20$ keV

(iii) Neon plasma sheath 0.4 torr

Shot 9904

6 cm

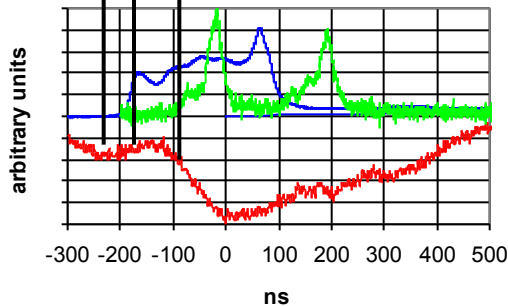


-242 ns

-182 ns

-82 ns

$n_e \approx 7 \times 10^{23} \text{ m}^{-3}$



Pinch phase ~ 200 ns before HXR and dl dip, $n_e \approx 1.6 \times 10^{24} \text{ m}^{-3}$

Duration of the stagnation 200 ns

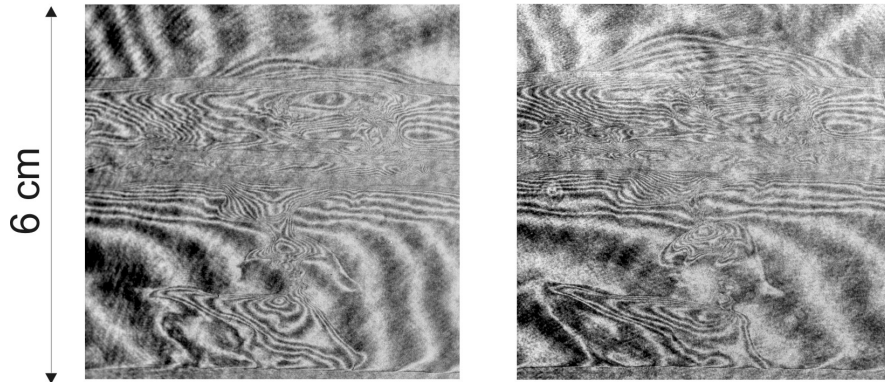
Length of the pinch 3 cm

Implosion velocity $2.25 \times 10^5 \text{ m/s}$; $E(\text{Ne}) \approx 2\text{-}3 \text{ keV}$

SXR, HXR, dl/dt

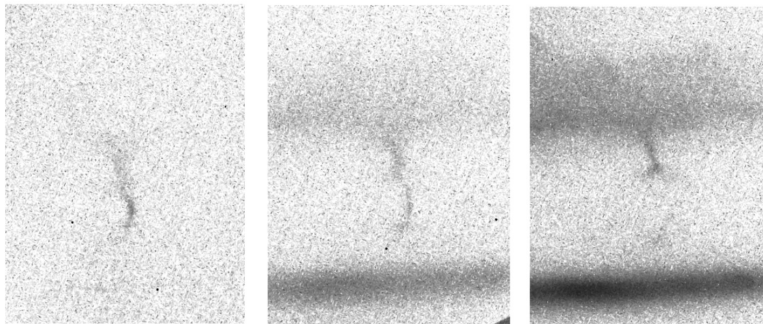
(iv) Neon plasma sheath + deuterium jet

Shot 9903



-54 ns

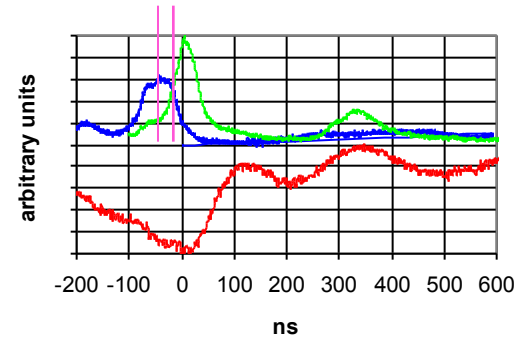
-34 ns



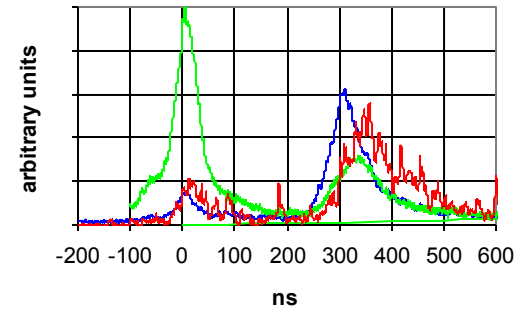
-50 ns

-40 ns

-30 ns



SXR, HXR, dI/dt



neutron signals down, side, up

NY 1×10^{10} , beam-target, $E_d(z) \approx 80$ keV, $E_d(r) \approx 20$ keV
Neutron production ≈ 200 ns after pinch at $n_e \approx 2 \times 10^{24} \text{ m}^{-3}$.

Comparisson of parameters in D and Ne

parameter	D/ 1.5torr	Ne/0.6 torr	Ne + D
Maximum of current [MA]	2.13	2.18	2.20
Implosion velocity of plasma sheath [$\times 10^5$ m/s]	2.4	2.2	2.2
Temporal position of the pinch toward the dip [ns]	0	-200 \pm 30	-200 \pm 30
n_e in pinch [$\times 10^{24}$ m $^{-3}$]	4.1	2.1	3.1
Current in pinch	1.44 \pm 0.1	1.69 \pm 0.1	1.66 \pm 0.1
Voltage peak	35.3	19.7	25
SXR FWHM [ns]	46	240	180
Total energy SXR Be 10 μ m \geq 700 eV [J]	1.1	2.8	1.0
Length of the column [cm]	6-8	3.2-3.4	3 cm
Ed(z)/Ed(r)	140/60		120/30
Implosion velocity of constriction [$\times 10^5$ m/s]	1.6		0.6
Energy of ions during constriction implosion [keV]	0.27		1.35

Thank you for your attention